Redox-Active Bisphosphonate-Based Viologens as Negolytes for Aqueous Organic Flow Batteries

Gabriel Gonzalez,[a] Anton A. Nechaev,[b]* Vsevolod A. Peshkov,[b] Eduardo Martínez-González,[a] Andrey Belyaev,[c] Mahsa Shahsavan,[a] Petri M. Pihko,[b]* Pekka Peljo[a]*

[a] Research Group of Battery Materials and Technologies, Department of Mechanical and Materials Engineering, Faculty of Technology, University of Turku, Turku, 20014, Finland

[b] Department of Chemistry, University of Jyväskylä, P. O. Box 35, Jyväskylä, 40014, Finland

[c] Department of Chemistry, University of Eastern Finland, Yliopistokatu 7, Joensuu, 80101, Finland

anton.a.nechaev@jyu.fi, petri.pihko@jyu.fi, pekka.peljo@utu.fi

Abstract

Viologen derivatives feature two reversible one-electron redox processes and have been extensively utilized in aqueous organic flow batteries (AOFBs). However, the early variant, methyl viologen (MVi), exhibits low stability in aqueous electrolytes, restricting its practical implementation in AOFB technology. In this context, leveraging the tunability of organic molecules, various substituents have been incorporated into the viologen core to achieve better stability, lower redox potential, and improved solubility. In this work, we introduce bisphosphonate-substituted viologens as candidates for AOFBs. The bulkiness and negative charges of the bisphosphonate groups enhance the solubility and the electrostatic repulsion among viologen molecules, minimizing the bimolecular side reactions that lead to degradation. Additionally, the electron-donating effect of this new substituent significantly lowers the redox potential. As a result, the proposed viologen derivatives exhibit high solubility (1.66 - 1.81 M in water) and stability (capacity decay of 0.009 %/cycle or 0.229%/day when tested at 0.5 M). These parameters are coupled with the lowest redox potentials exceeding all previously reported viologens utilized in AOFBs (–0.503 V and –0.550 V against SHE for mono- and bis-phosphonate viologen, respectively).

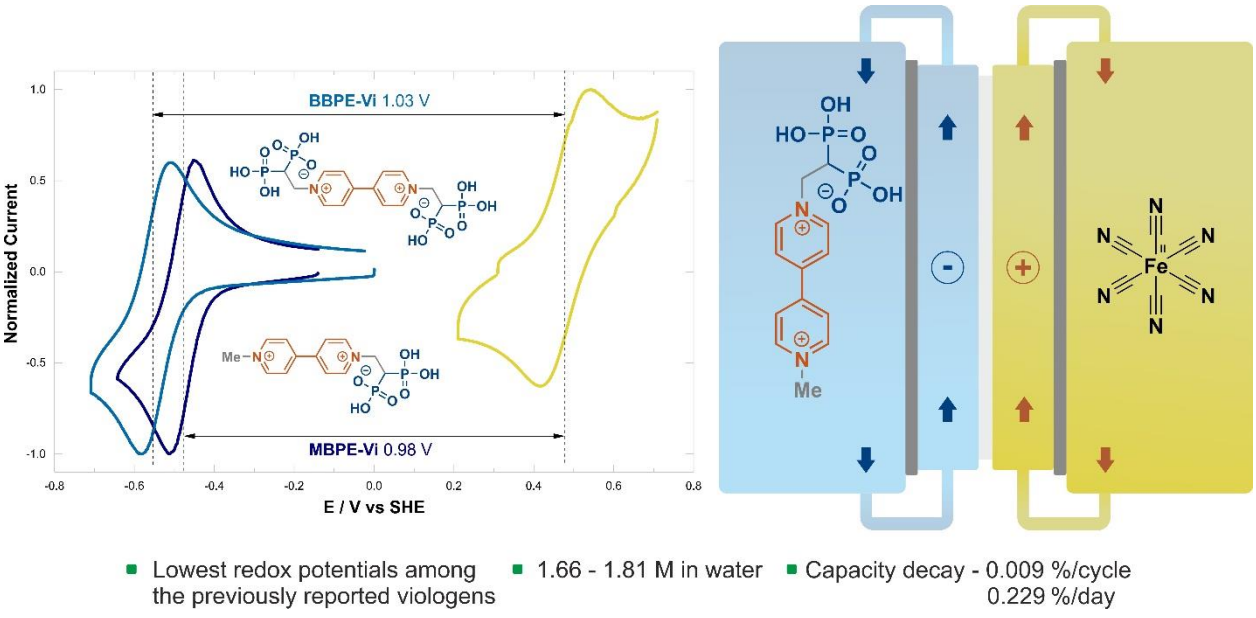

Introduction

Our society faces an urgent demand for realizing sustainable energy infrastructure to mitigate climate change by reducing carbon dioxide emissions. This includes decreasing the dependence on fossil fuel-based energy resources and transitioning towards a cleaner and more resilient ways of energy generation.[1–3] In this regard, the energy extracted from the Earth's crust, moving water, solar light, and wind meets the requirements of energy production with the minimal carbon emission. However, the use of geothermal energy and hydroelectricity is restricted by the availability of specific geographical conditions, while in case of wind[4] and solar[5] energy, dependency on weather conditions requires cost-effective and long-lasting energy storage solutions.

Flow batteries (FBs) offer a promising avenue to address the intermittent nature of renewable energy sources and the increasing demand for grid-scale energy storage at the time scale of hours up to ca. a week.[6,7] Unlike conventional batteries, which store energy in solid materials, FBs store energy in liquid electrolytes, enabling scalable and customizable energy storage capacities.[8] The most developed system corresponds to vanadium flow battery (VFB),[9] which is currently being widely deployed on a large scale.[10] However, the application of this technology for large-scale stationary systems faces some challenges, mainly related to the availability and high cost of vanadium, and the acidity and toxicity of the electrolytes.[11,12] In this regard, the utilization of organic molecules in aqueous organic flow batteries (AOFB) has emerged as a promising alternative.[13] The primary benefit on using organic materials is that they can be synthetized from natural sources, leading to scalable and cost-effective storage systems. Furthermore, a key advantage of incorporating organic molecules into FBs is the possible wide range of parameters, which can be tailored by modifying their chemical structure. This tunability allows for the design of materials with desired redox potentials and solubility, enhancing the flexibility and performance of FB systems.[14–16]

After Liu and coworkers reported the first fully AOFB utilizing methyl viologen (**MVi**) and 4-hydroxy-2,2,6,6-tetramethylpiperidin-1-oxyl (4-HO-TEMPO) in 2016,[17] a wide variety of water-soluble electroactive materials have been explored[18,19] with viologen derivatives being extensively utilized as the negative anolyte (negolyte).[20] However, cross-contamination through membrane as well as amplification of undesired reactivity with the concentration increase persist as major problems leading to reduced performance of viologen-based FB.[21] Ideally, a molecule intended for FBs should possess zwitterionic nature and be sufficiently bulky to prevent crossover through an ion-exchange membrane. The latter criterion is also beneficial from a viewpoint of minimizing collisions among redox-active molecules, thus preventing degradation via unwanted chemical side-reactions.[22]

Due to the high solubility and two reversible one-electron redox processes, extensive research work has been conducted for the deployment of viologen derivatives as negolytes for AOFBs. Table S2 in the Supporting Information summarizes the parameters of the main viologens, including different substituents, that have been considered for AOFB application. In 2017, Aziz and co-workers incorporated positively charged ammonium groups to the viologen core and demonstrated the high performance of the new derivative, **BTMAP-Vi**, in a neutral-pH AOFB.[23] The positive charges enhance electrostatic repulsion between viologen molecules in the electrolyte preventing disproportionation and side reactions, as well as they substantially reduced the permeability through the ion-exchange membrane. As a result, **BTMAP-Vi** exhibited a mayor improvement, compared with **MVi**, when tested in a flow cell (capacity decay of 0.1 %/day against with 3.5 % of **MVi**). Despite the higher stability, **BTMAP-Vi** presents less negative redox potential than **MVi** (–0.358 V against –0.420 V of **MVi**, reported against

SHE) because of the electron-withdrawing nature of the ammonium groups, leading to lower cell voltage. Later, in 2020, Aziz´s group presented a near-neutral-pH AOFB featuring 1,1'-bis(3-phosphonopropyl)-viologen (**BPP–Vi**) as a negolyte.[24] The inclusion of negatively charged phosphonate groups resulted in extremely low capacity decay (0.016 % per day) coupled with a reduction of the redox potential (–0.462 V vs SHE). Table 1 summarizes the results obtained for these viologens including the mentioned substituents and a comparison with the simplest form, **MVi**.

Table 1: Summary of reported Viologen derivatives used in AOFBs.

Viologen derivative	Chemical structure	Redox Potential vs SHE / V	Maximum Solubility	Stability (concentration of Vi and electrolyte)	Comments
MVi [17]	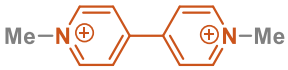	–0.420	2.5 M in water 2.4 M in 1.5 M NaCl	0.12 %/cyc 3.5 %/day (0.5 M in 1.5 M NaCl)	High permeation and fast bimolecular decomposition
BTMAP-Vi [23]	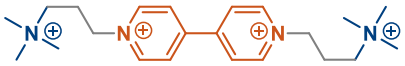	–0.358	2 M in water	0.0057 %/cyc 0.1 %/day (1.3 M in water)	Less negative redox potential compared with MVi
BPP-Vi[24]	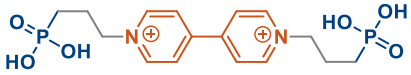	–0.462	1.23 M in water	0.00069 %/cyc 0.016 %/day (1 M titrated with NH_4OH 14 M to pH 9)	Overcharge leads to increased capacity fade

In this work, we introduce 1,1'-bis(2,2-bisphosphonoethyl)-viologen (**BBPE–Vi**) and 1-methyl-1'-(2,2-bisphosphonoethyl)-viologen (**MBPE–Vi**) as a new class of AOFB active molecules to explore how the electrochemical properties of viologens are affected if bisphosphonate fragment is introduced instead of monophosphonate on the alkyl chain of the 4,4-dipyridil core of **BPP–Vi**. Geminal bisphosphonates or simply bisphosphonates are defined by a bulky branched structure and are well known for their pharmaceutical applications in treating bone-related diseases.[25,26] The P–C–P bonds in the bisphosphonate exhibit stability against heat and most chemical reagents and remain entirely resistant to enzymatic hydrolysis.[27] With these distinctive properties, sterically hindered bisphosphonates might possess significant untapped potential for integration into FB technology.

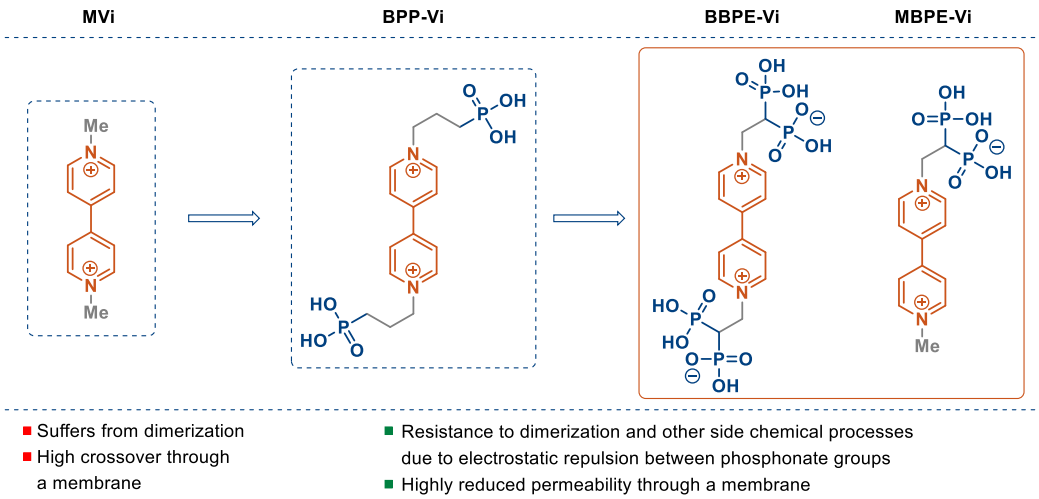

Scheme 1. Design of bisphosphonate-based viologen molecule for AORFB

Synthesis and XRD studies of bisphosphonate-based viologens

The synthesis of symmetric 1,1′-bis(2,2-bisphosphonoethyl)-viologen (**BBPE–Vi**) was achieved by a double aza-Michael addition of commercial 4,4-dipyridyl to ethene-1,1-diylbis(phosphonic acid) (**1**). The reaction took place in water at 100°C, delivering **BBPE–Vi** in excellent yield (85%, see Scheme 2).[28] The required bisphosphonic acid **1** was prepared using a slightly modified version of the previously described procedure.[29] A mono methylated dipyridyl derivative **2** was obtained by alkylating 4,4-dipyridyl first with methyl iodide. Subjecting **2** to the aza-Michael reaction produced the non-symmetric 1-methyl-1′-(2,2-bisphosphonoethyl)-viologen (**MBPE–Vi-I**) featuring iodide as the counterion in good yield (68%). Treating **2** with Amberlite 900 Cl^- ion-exchange resin followed by aza-Michael addition to **1** delivered chloride form **MBPE–Vi-Cl** in an overall yield of 67% (Scheme 2).

The structure of **MBPE–Vi-Cl** (Scheme 2, Figure S1, Table S1) was elucidated by single-crystal X-ray diffraction (SC-XRD) analysis. Hygroscopic needle-like crystals were obtained by slow diffusion of methanol into an aqueous solution of **MBPE–Vi-Cl**. Key structural parameters such as P–O, N–C, and P–C bond lengths and angles are consistent with previously reported data[29]. An intriguing aspect of this structure is the formation of polymeric two-dimensional heterolayers (Figure S4). In this arrangement, the bisphosphonate fragments adopt a head-to-head orientation, resulting in a densely packed layer with an average thickness of 4.35–4.47 Å, while the methyl bipyridyl tails and chloride counterions extend outward from the layer. An attempt to crystallize **MBPE–Vi-I** led to the formation of two other forms that we were able to confirm via SC-XRD analysis: triiodide **MBPE–Vi-I3** and zwitterionic form **MBPE–Vi-ZI** (Scheme 2, Figure S2-3). This transformation is attributed to the slow oxidation of iodine that occurs during the exposure of **MBPE–Vi-I** solution to air [29]. The viologen cation in **MBPE–Vi-I3** adopts a twisted configuration with a dihedral angle of 21.6°, while the I_3^- counterion aligns along the bipyridine core, forming a contact ion pair with intramolecular distances of 3.973(2)–4.095(6) Å. Similar to the chloride viologen, the **MBPE–Vi-I3** molecules exhibit a head-to-head organization, forming a two-dimensional layered framework via extended hydrogen bonding between bisphosphonate fragments, resulting in an almost doubled sheet thickness (Figure S5). Both iodide and chloride forms of **MBPE-Vi** showed similar electrochemical behavior under the oxygen-free conditions. However, most of the electrochemical measurements were conducted with **MBPE–Vi-I** due to the ease of its preparation.

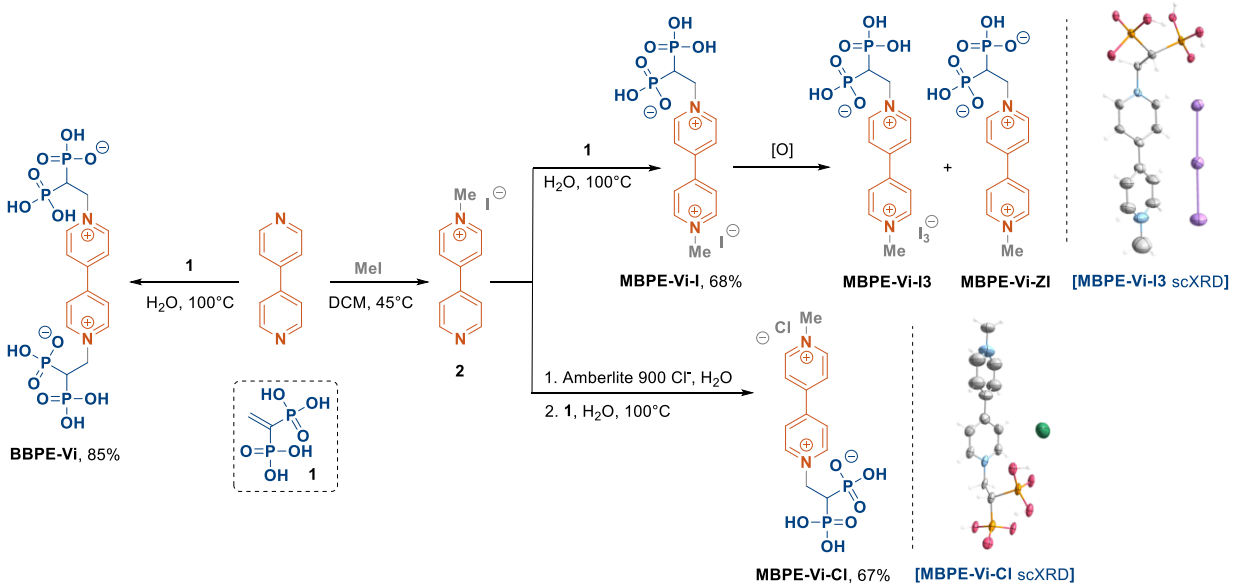

Scheme 2. Synthesis of 1,1′-bis(2,2-bisphosphonoethyl)-viologen **BBPE–Vi** and 1-methyl-1′-(2,2-bisphosphonoethyl)-viologen **MBPE–Vi**

Electrochemical studies of bisphosphonate-based viologens

Cyclic voltammetry measurements were performed to study the reversibility and redox potential of **BBPE-Vi** and **MBPE-Vi** in aqueous electrolytes, using neutral and basic electrolytes (1 M KCl and 0.1-1 M NaOH). The cyclic voltammograms, presented in the Supporting information S3, show the two one-electron-processes characteristic of viologens, with an increased reversibility at higher pH. In this discussion, we limit the analysis to the first electron as the species generated from the second reduction (Vi^0) shows low stability in aqueous electrolytes.[30–32] Figure 1A shows the highly reversible first redox reaction of the mono-substituted viologen **MBPE-Vi** in 0.1 M NaOH, while the bi-substituted form **BBPE-Vi** requires a higher basicity to achieve a reversible behaviour (1 M NaOH). Regarding the redox potentials, we can observe an improvement on the values obtained for both bisphosphonate-substituted viologens, –0.503 V for **MBPE-Vi** while –0.550 V for **BBPE-Vi** (against SHE), confirming the higher electron-donating strength of the proposed functional group (Figure 1A). The bi-substituted form achieves a decrease of 120 and 88 mV when compared with the reduction potentials of **MVi** and **BPP-Vi**, respectively, leading to the most negative potential reported among viologen derivatives. By coupling **BBPE-Vi** with ferrocyanide on the positive side, a cell with an open circuit voltage over 1 V can be obtained (see Figure 1A-B).

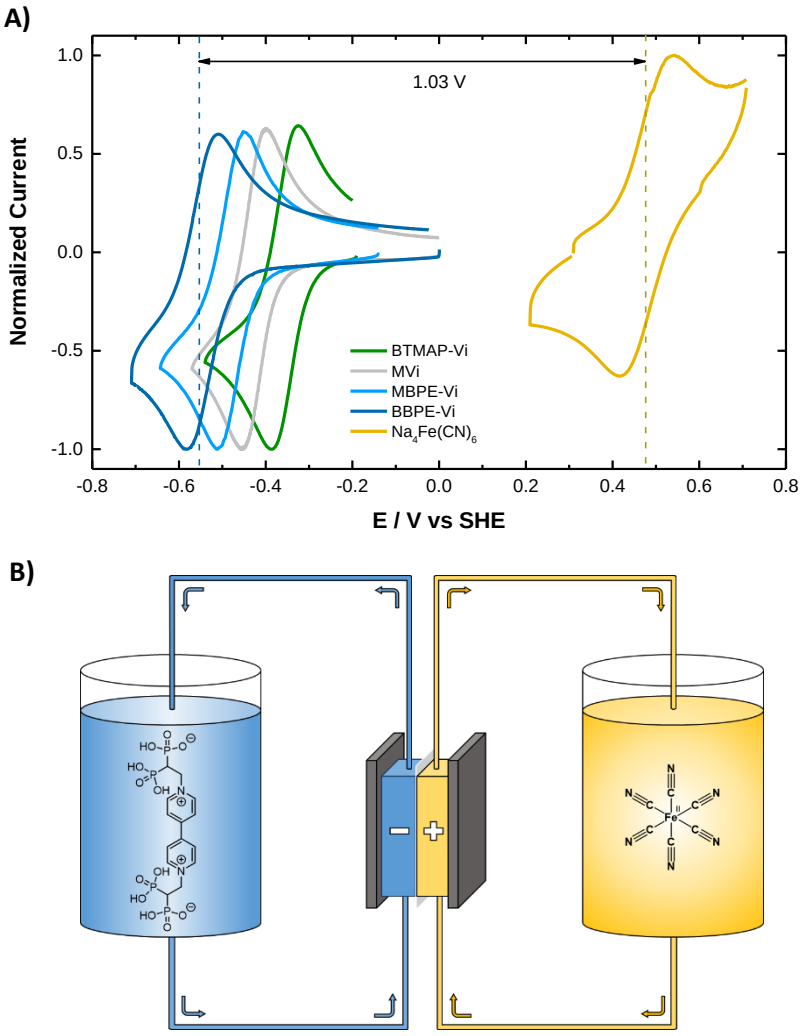

Figure 1: **A)** Cyclic voltammograms of **BBPE-Vi** and **MBPE-Vi** compared against previously reported viologen derivatives. Cell voltage of **BBPE-Vi** when coupled with ferrocyanide. CV conditions: 1 mM **BBPE-Vi** in 1 M NaOH; 5 mM **MBPE-Vi** in 0.1 M NaOH; 1.2 mM **MVi** in acetate buffer 0.5 M; 1 mM **BTMAP-Vi** in 1 M KCl, 1 mM $Na_4Fe(CN)_6$ in 0.1 M NaOH. Scan rate: 100 mV s^{-1}. **B)** Scheme of a flow cell assembled with **BBPE-Vi** and ferrocyanide.

We next evaluated the performance of the viologen derivatives in lab-scale flow cells paired with ferrocyanide as posolyte. The experiments were performed in a nitrogen-filled glovebox using a 5 cm^2 battery with cationic exchange membrane Nafion 212. Further description of the battery tests is presented in Supporting Information S4. First, we used low concentrations of Vi (5-10 mM) with an excess amount of posolyte. **BBPE-Vi** was tested in a cell using 5 mM concentration in 1 M NaOH as supporting electrolyte considering that more alkalinity was required to obtain reversible behaviour during the cyclic voltammetry measurements. The battery accessed 70% of the total capacity when cycling at 1 mA cm^{-2} with a cut-off voltage of 1.02 V, exhibiting a capacity decay of 0.166 %/cycle (see Supporting Information S4.1). We assume that the considerable capacity fade arises from the higher alkalinity of the electrolyte, as a result of the dealkylation of the viologen core generated by the nucleophilic attack of the hydroxide anions. This accelerated degradation of viologens in strongly alkaline electrolytes has been previously reported in the literature.[33]

The battery tests of **MBPE-Vi** were performed with a concentration of 10 mM using 0.1 M NaOH as supporting electrolyte, exhibiting a higher stability when compared with bi-substituted form **BBPE-Vi**. The battery demonstrated an increase on the stability when using lower cut-off voltages while achieving lower capacity utilization (see Supporting Information S4.2). Using a cut-off voltage of 0.90 V with 50% capacity utilization did not exhibit a visible fade rate, while increasing the cut-off to 1.00 V with 95% capacity utilization leads to a capacity decay of 0.09 %/cycle (see Supporting Information S4). A longer cycling using a cut-off voltage of 0.925 V (72% of capacity utilization), exhibited a fade rate of 0.042 %/cycle over 100 cycles. We assume that the lower stability when using higher cut-offs arises from partially accessing the double reduced form that is unstable in aqueous electrolytes. Previous works demonstrated that MVi^0 (neutral viologen generated after two-electron reduction) is irreversibly protonated by water to generate inactive redox species.[30–32] A similar behaviour was described by Aziz when overcharging **BBP-Vi**[24]. We next performed a test utilizing a cut-off voltage of 1.30 V in order to cycle the second electron, obtaining a much lower stability (decay of 2.03 %/cycle) that supports our assumption. This observation suggests that the cycling stability of the first electron is affected by the assessment of the second reduced species and, as a result, by the separation between the redox potentials of the first and second redox processes. The comparison of the viologens presented in Table S2 in the Supporting Information is in agreement with our hypothesis: while **MVi** and **BBPE-Vi** present the lowest stabilities with separations of 0.31 and 0.32 V between the redox processes, respectively, **BPP-Vi** and **Dex-Vi** exhibit the most stable operations with larger separations of 0.39 and 0.38 V, respectively. However, we understand that there are other factors contributing to the measured stability (electrolyte pH, viologen concentration and stability of the double reduced species) and further investigations are required for validation. Finally, we assembled a cell using 5 mM of mono-substituted viologen **MBPE-Vi** in 1 M NaOH as supporting electrolyte. The battery exhibited three times higher capacity decay (0.137 %/cycle) than in 0.1 M NaOH when cycling 71% of the full capacity (cut-off voltage of 0.95 V), confirming our previous assumption that the studied viologen derivatives decompose at higher rate in highly alkaline conditions when cycled in a battery.

We continued our studies with **MBPE-Vi** because of its higher stability. To characterize the reduced species of **MBPE-Vi**, UV-Vis measurements were carried out. The reduced forms were electro-generated in a flow cell by charging with the corresponding cut-off voltage (see Supporting Information, S5). The first reduction to obtain the radical **MBPE-Vi$^{\bullet}$** was confirmed by the UV-Vis spectrum, which exhibited two main peaks characteristic of viologen radicals at 400 and 600 nm.[30,34,35] Furthermore, we measured the absorbance spectra after charging at higher cut-off voltage for one and two electrons. The one-electron reduction sample generated using higher cut-off voltage shows an increase on the absorption

peak attributed to the second reduced species. This is in agreement with the battery tests results discussed previously: the second electron is already accessed when conducting the first-electron reduction using higher cell voltage, which results on higher decomposition rate. Finally, the samples were stored inside the glovebox and the absorbance was measured over time for 12 days to study their stability. The UV-Vis results confirmed the much higher stability of the first reduced species when compared with the double-reduced form, which appears to decompose totally after four days.

To further characterize **MBPE-Vi**, we performed cyclic voltammetry measurements at different scan rates to determine the diffusion coefficient (D) and rate constant (k^0) of the first redox process. The voltammograms and calculations are presented in the Supporting Information, sections S7 and S8. The diffusion coefficient D, calculated using Randles-Ševčík equation, was estimated as 3.91 10^{-6} cm^2 s^{-1}, within the range of the values reported for other studied viologens (3-6 10^{-6} cm^2 s^{-1}).[36] The rate constant k^0 was calculated using Marcus-Hush approximation suggested by E. González[37] obtaining 0.13 cm s^{-1}. This value corresponds to fast kinetics, comparable with the rate constants of previous reported viologens,[36] indicating that the inclusion of the suggested bisphosphonate groups brings on thermodynamic benefits, as high solubility and lower redox potential, while not significantly altering the kinetic component. We conducted the same characterization for the bi-substituted viologen **BBPE-Vi**, resulting on a diffusion coefficient of 1.47 10^{-6} cm^2 s^{-1} and a rate constant of 0.025 cm s^{-1}. In this case, we believe that the calculated diffusion coefficient D is undersestimated considering the quasi-reversible behaviour of **BBPE-Vi** and the lower accuracy of the Randles-Ševčík approach for those cases. Finally, we estimated the maximum solubility of **MBPE-Vi** in water in the range of 1.66 - 1.81, which corresponds to a volumetric capacity of 44.9 – 48.5 Ah L^{-1}.

The flow cell tests with higher **MBPE-Vi** concentration were performed assuming that deprotonation of the three protons of the bisphosphonate group is essentially complete. This assumption was based on the pK_a values reported for biphosphonic acids.[38] Even though the acidity constants have not been determined for viologen bisphosphonate, we surmise that the pK_as of **MBPE-Vi** should be lower than those determined for the corresponding $CHCH_3$ bisphosphonate, which presents pK_a values of 2.73, 7.05 and 11.59.[38] In our case, in order to hold a pH level of 13, a higher concentration of NaOH was used. The high concentration battery was then assembled using 0.5 M of **MBPE-Vi** dissolved in NaOH 1.6 M. The pH of the electrolyte was 9.8 after dissolving **MBPE-Vi**, after which the pH was adjusted to 13.5. The positive side consisted on an excess amount of a mixture of potassium ferro- and ferricyanide The battery was cycled with the constant current protocol (CC) for over 200 cycles at 40 mA cm^{-2} with a cut-off voltage of 1.02 V accessing 64% of the theoretical capacity. In that condition, the cell exhibit a high stability with a capacity decay of 0.009 %/cycle (0.229 %/day) and coulombic and energy efficiencies of 99.98 % and 81 %, respectively (see Figure 2). We believe that the fluctuation on the discharge capacity during cycling (Figure 2B) is linked to the glovebox temperature changes and the use of CC protocol. This effect, described by Fell,[39] arises from the electrolyte and membrane conductivity changes at different temperature and determines the capacity accessed in each cycle when using a CC protocol. Furthermore, we attribute a small contribution of the capacity decay to the solubility of potassium ferrocyanide, which was confirmed by the increase of the capacity accessed at cycle 171 when adding supporting electrolyte to the posolyte tank. Finally, we performed a short cycling at 20 and 40 mA cm^{-2}, obtaining high energy efficiency values of 88 and 80% (Figure 3C), which are consistent with the calculated high-rate constant. Once the battery was stopped, we conducted cyclic voltammetry measurements of the electrolytes after cycling (presented in the Supporting Information). The voltammograms, after over 27-days-cycling, did not show any indication of crossover of the active species through the membrane, which confirms the low permeability of the **MBPE-Vi**.

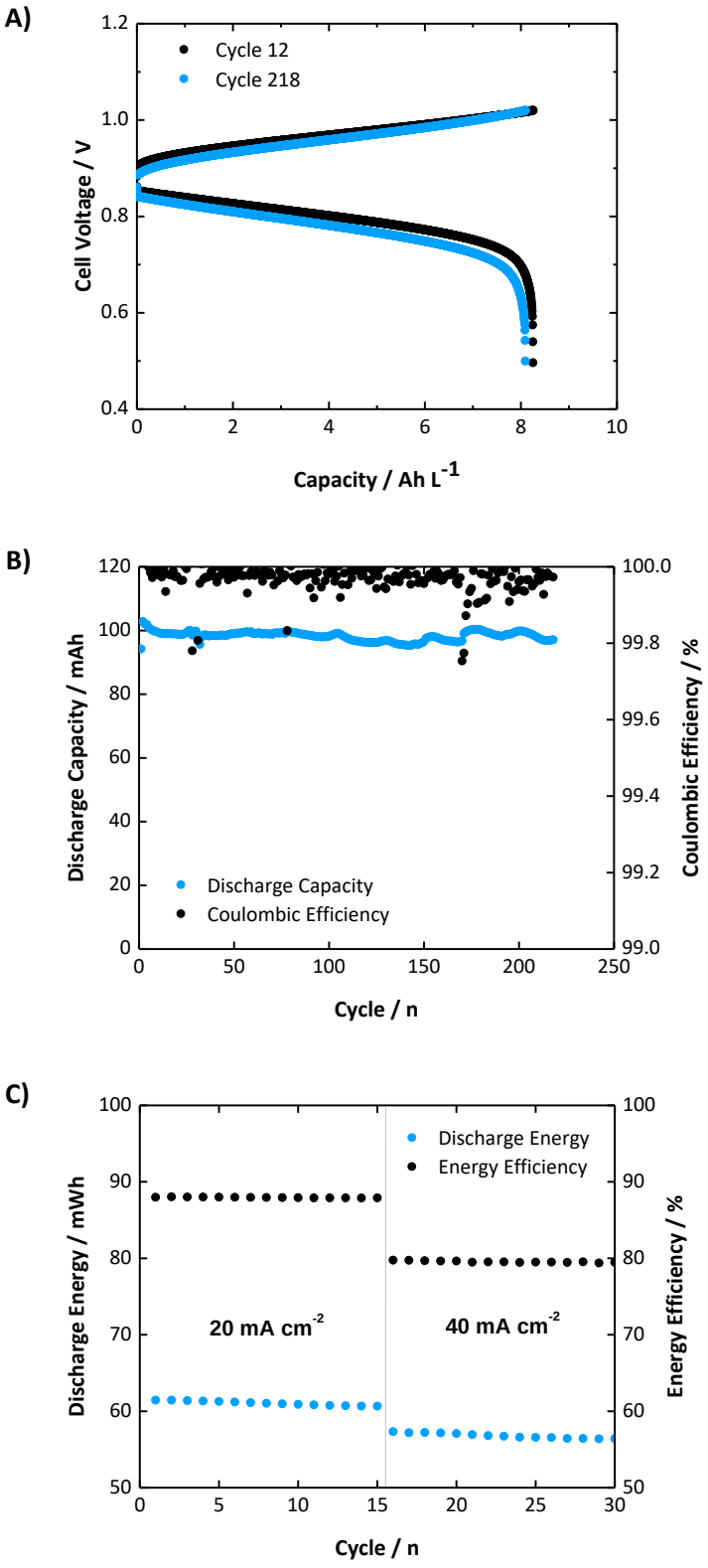

Figure 2: **MBPE-Vi** 0.5 M flow cell performance. Supporting electrolyte: 1.6 M NaOH. Positive side: $Na_4Fe(CN)_6$ 0.5 M (excess amount) **A)** Charge-discharge profiles of cycles 12 and 218. **B)** Capacity and coulombic efficiency evolution. **C)** Energy capability and efficiency at different current densities.

Conclusions

In this work, we explored the electrochemistry of two novel viologen derivatives featuring bisphosphonate group on their *N*-alkyl chain. The negatively charged oxygen atoms of bisphosphonate

groups enable high solubility in aqueous electrolyte while their electron-donating effect is advantageous for achieving very low redox potentials. In particular, one of the obtained derivatives **BBPE-Vi** exhibited the most negative potential reported among all viologens used in AOFBs, leading to a cell voltage over 1 V when coupled with ferrocyanide. Another derivative **MBPE-Vi** had a slightly higher potential while showing better performance in battery tests. A flow cell with 0.5 M of **MBPE-Vi** demonstrated good stability (capacity decay of 0.009 %/cycle, 0.229%/day) with high coulombic (99.98%) and energy efficiency (81%) when cycled at 40 mA cm^{-2}. Although the decomposition rate was found to increase when moving towards a full charge of the active material, the high solubility of our molecules (up to 1.81 M) still allows achieving substantial energy storage capacity even with reduced capacity utilization (34.0 Ah L^{-1} operating at 70% of the full capacity). These findings underscore the importance of precise molecular design in developing new organic negolytes with high solubility and low redox potential, paving the way for organic flow batteries with competitive energy and power density.

Acknowledgments

This project has received funding from the European Union's Horizon2020 Research and Innovation programme under grant agreement No 875565 (Project CompBat). Support from Research Council Finland (project 348328 - via European Union – NextGenerationEU instrument - to P.M.P.) and 346895 (to A. N.) is gratefully acknowledged. P.P. gratefully acknowledges the Academy Research Fellow funding (grant no. 315739, 343791, 320071 and 343794) and BioFlow project (grant no. 343493) from Research Council Finland, and European Research Council through a Starting grant (agreement no. 950038). We also thank Dr. Anniina Kiesilä for assistance with mass spectrometry. We also acknowledge Ali Tuna and Jenni Jarju for the collaboration on NMR spectrometry studies.

References

[1] D. Larcher, J.-M. Tarascon, *Nat Chem* **2015**, *7*, 19–29.

[2] K. Moustakas, M. Loizidou, M. Rehan, A. S. Nizami, *Renewable and Sustainable Energy Reviews* **2020**, *119*, 109418.

[3] R. Eisenberg, H. B. Gray, G. W. Crabtree, *Proceedings of the National Academy of Sciences* **2020**, *117*, 12543–12549.

[4] M. A. Hannan, A. Q. Al-Shetwi, M. S. Mollik, P. J. Ker, M. Mannan, M. Mansor, H. M. K. Al-Masri, T. M. I. Mahlia, *Sustainability* **2023**, *15*, 3986.

[5] H. H. Pourasl, R. V. Barenji, V. M. Khojastehnezhad, *Energy Reports* **2023**, *10*, 3474–3493.

[6] P. Arévalo-Cid, P. Dias, A. Mendes, J. Azevedo, *Sustain Energy Fuels* **2021**, *5*, 5366–5419.

[7] J. Luo, B. Hu, M. Hu, Y. Zhao, T. L. Liu, *ACS Energy Lett* **2019**, *4*, 2220–2240.

[8] Z. Yang, J. Zhang, M. C. W. Kintner-Meyer, X. Lu, D. Choi, J. P. Lemmon, J. Liu, *Chem Rev* **2011**, *111*, 3577–3613.

[9] K. Lourenssen, J. Williams, F. Ahmadpour, R. Clemmer, S. Tasnim, *J Energy Storage* **2019**, *25*, 100844.

[10] Z. Lv, X. Sun, M. Xu, C. Lin, J. Guo, M. Wang, X. Liu, in *Proceedings of the 3rd International Conference on Big Data Economy and Information Management, BDEIM 2022, December 2-3, 2022, Zhengzhou, China*, EAI, **2023**.

[11] J. Luo, A. P. Wang, M. Hu, T. L. Liu, *MRS Energy & Sustainability* **2022**, *9*, 1–12.

[12] A. G. Olabi, M. A. Allam, M. A. Abdelkareem, T. D. Deepa, A. H. Alami, Q. Abbas, A. Alkhalidi, E. T. Sayed, *Batteries* **2023**, *9*, 409.

[13] J. Winsberg, T. Hagemann, T. Janoschka, M. D. Hager, U. S. Schubert, *Angewandte Chemie International Edition* **2017**, *56*, 686–711.

[14] Y. Ding, C. Zhang, L. Zhang, Y. Zhou, G. Yu, *Chem Soc Rev* **2018**, *47*, 69–103.

[15] P. Leung, A. A. Shah, L. Sanz, C. Flox, J. R. Morante, Q. Xu, M. R. Mohamed, C. Ponce de León, F. C. Walsh, *J Power Sources* **2017**, *360*, 243–283.

[16] X. Wang, R. K. Gautam, J. "Jimmy" Jiang, *Batter Supercaps* **2022**, *5*, DOI 10.1002/batt.202200298.

[17] T. Liu, X. Wei, Z. Nie, V. Sprenkle, W. Wang, *Adv Energy Mater* **2016**, *6*, DOI 10.1002/aenm.201501449.

[18] Z. Li, T. Jiang, M. Ali, C. Wu, W. Chen, *Energy Storage Mater* **2022**, *50*, 105–138.

[19] G. Yang, Y. Zhu, Z. Hao, Y. Lu, Q. Zhao, K. Zhang, J. Chen, *Advanced Materials* **2023**, *35*, DOI 10.1002/adma.202301898.

[20] M. Kathiresan, B. Ambrose, N. Angulakshmi, D. E. Mathew, D. Sujatha, A. M. Stephan, *J Mater Chem A Mater* **2021**, *9*, 27215–27233.

[21] Y. Cho, H. Kye, B.-G. Kim, J. E. Kwon, *Journal of Industrial and Engineering Chemistry* **2024**, *136*, 73–88.

[22] X. Fang, Z. Li, Y. Zhao, D. Yue, L. Zhang, X. Wei, *ACS Mater Lett* **2022**, *4*, 277–306.

[23] E. S. Beh, D. De Porcellinis, R. L. Gracia, K. T. Xia, R. G. Gordon, M. J. Aziz, *ACS Energy Lett* **2017**, *2*, 639–644.

[24] S. Jin, E. M. Fell, L. Vina-Lopez, Y. Jing, P. W. Michalak, R. G. Gordon, M. J. Aziz, *Adv Energy Mater* **2020**, *10*, DOI 10.1002/aenm.202000100.

[25] Z. A. Habib, *Expert Rev Endocrinol Metab* **2017**, *12*, 59–71.

[26] J. S. Barbosa, S. S. Braga, F. A. Almeida Paz, *Molecules* **2020**, *25*, 2821.

[27] *Principles of Bone Biology*, Elsevier, **2008**.

[28] Y. Zhang, A. Leon, Y. Song, D. Studer, C. Haase, L. A. Koscielski, E. Oldfield, *J Med Chem* **2006**, *49*, 5804–5814.

[29] J. Desai, Y. Wang, K. Wang, S. R. Malwal, E. Oldfield, *ChemMedChem* **2016**, *11*, 2205–2215.

[30] J. W. Park, J. H. Kim, B. K. Hwang, K. K. Park, *Chem Lett* **1994**, *23*, 2075–2078.

[31] J. Y. Kim, C. Lee, J. W. Park, *Journal of Electroanalytical Chemistry* **2001**, *504*, 104–110.

[32] M. Venturi, Q. G. Mulazzani, M. Z. Hoffman, *J Phys Chem* **1984**, *88*, 912–918.

[33] R. Rubio-Presa, L. Lubián, M. Borlaf, E. Ventosa, R. Sanz, *ACS Mater Lett* **2023**, *5*, 798–802.

[34] T. M. Bockman, J. K. Kochi, *J Org Chem* **1990**, *55*, 4127–4135.

[35] K. Madasamy, V. M. Shanmugam, D. Velayutham, M. Kathiresan, *Sci Rep* **2018**, *8*, 1354.

[36] Y. Liu, Q. Chen, P. Sun, Y. Li, Z. Yang, T. Xu, *Mater Today Energy* **2021**, *20*, 100634.

[37] E. Martínez-González, H. G. Laguna, M. Sánchez-Castellanos, S. S. Rozenel, V. M. Ugalde-Saldivar, C. Amador-Bedolla, *ACS Appl Energy Mater* **2020**, *3*, 8833–8841.

[38] P. Haratipour, C. Minard, M. Nakhjiri, A. Negahbani, B. T. Chamberlain, J. Osuna, T. G. Upton, M. Zhao, B. A. Kashemirov, C. E. McKenna, *J Org Chem* **2020**, *85*, 14592–14609.

[39] E. M. Fell, M. J. Aziz, *J Electrochem Soc* **2023**, *170*, 100507.